Journal of ELECTRONIC MATERIALS, Vol. 49, No. 5, 2020
https://doi.org/10.1007/s11664-020-07991-5

TOPICAL COLLECTION: INTERNATIONAL CONFERENCE ON THERMOELECTRICS 2019

The High Potential for Waste Heat Recovery in Hybrid Vehicles: A Comparison Between the Potential in Conventional and Hybrid Powertrains

MARTIN KOBER [1,2]

1.—German Aerospace Center (DLR), Institute of Vehicle Concepts, Pfaffenwaldring 38-40, 70569 Stuttgart, Germany. 2.—e-mail: martin.kober@dlr.de

In future mobility, the mix of different drive trains will probably be much more diverse than it is today. According to a large number of scenario analyses, a predominant number of vehicles will continue to be based on the internal combustion engine (ICE), while an increasing number of hybrid vehicles are expected. To achieve the required reductions in CO_2 emissions it is necessary to investigate all potential technologies for efficiency improvement. Therefore in this work the potential of waste heat recovery is examined for conventional and hybrid vehicles. Due to the fact that in an internal combustion engine approximately 2/3 of the fuel's chemical energy dissipates as waste heat, the potential for the recovery of this energy in all ICE driven powertrains is, in principle, high. The results of this work show that in hybrid vehicles the highest share of the energy supplied by the fuel is lost in the exhaust gas. In order to further elaborate this result, we conduct an exemplary examination of two comparable vehicles of the compact class within the worldwide harmonized light duty test cycle. Measurement data from the two vehicles at the roller dynamometer is used. The result shows that the averaged exhaust gas heat flow of the conventional vehicle is 5.0 kW. For the hybrid vehicle, driving in the charge sustaining mode, the averaged exhaust gas heat flow results in 8.1 kW. The comparison shows that the temperature level of this exhaust gas is even higher than that of the conventional vehicle. In addition, this work shows that through the higher temperatures, the exergy in the exhaust gas is higher in hybrid vehicles even if the combustion engine works with a higher efficiency. In the exemplary comparison the averaged exergy of the exhaust gas is 3.2 kW for the conventional and 5.7 kW for the hybrid vehicle. As a result of this work, the high potential for waste heat recovery in hybrid vehicles could be demonstrated.

Key words: Waste heat recovery, conventional and hybrid powertrains, thermoelectric generator, power generation, exergetic potential

List of Symbols

c_p	Specific heat capacity (J/kg K)
E	Exergy flow (W)
h	Heat of combustion (J/kg)
m	Mass (kg)
$\dot{m}$	Mass flow (g/s)
p	Pressure (Pa)
$\dot{Q}$	Heat flow (W)
T	Temperature (K)
U	Internal energy (J)
V	Volume (dm^3)
η_C	Carnot efficiency (−)
φ	Crank angle (°)

Abbreviations

CO_2	Carbon dioxide
DLR	Deutsches Zentrum für Luft- und Raumfahrt/German Aerospace Center

(Received August 21, 2019; accepted January 31, 2020; published online February 13, 2020)

DSG	Dual-clutch gearbox
ICE	Internal combustion engine
ORC	Organic Rankine cycle
PHEV	Plug-in hybrid
TEG	Thermoelectric generator
TEM	Thermoelectric module
TSI	Turbocharged stratified injection
WLTC	Worldwide harmonized light duty driving test cycle
WLTP	Worldwide harmonized light duty vehicles test procedure

Indexes

A	Ambient
CO	Coolant
F	Fuel
HG	Hot gas
I	In
Leak	Leakage
max	Maximum
mi	Average
O	Out
W	Wall

INTRODUCTION

One of the major challenges for future automotive development is to achieve the required reductions of the CO_2 emissions. Therefore, it is necessary to investigate all potential technologies for efficiency improvement. In an internal combustion engine (ICE) approximately 2/3 of the fuel's chemical energy dissipates as waste heat. In particular, the exhaust gas offers the highest potential for waste heat recovery due to its high temperature level. One of the promising technologies for automotive waste heat recovery is the use of thermoelectric generators (TEG). Therefore this technology has been under investigation for several years at the DLR—Institute of Vehicle Concepts in Stuttgart.[1–5]

According to the majority of current scenario analyses, it is to be expected that the majority of new registrations in the future will continue to be based on an internal combustion engine. It is assumed that in 2030 this share will account for more than 80% and in 2040 more than 70% of new registrations. In addition, an increasing number of these vehicles with ICEs will be hybrid vehicles.[6,7] According to Ref. 7, which gives a summary of the literature, global car sales in 2030 are expected to be about 150% of the sales in 2015. This leads to the prediction that, in absolute terms, more vehicles with combustion engines will be sold in 2030 than are sold today.[7]

The aim of this paper is to consider future influences of development in the vehicle sector of potential waste heat recovery. In particular, the difference between conventional and hybrid vehicles was investigated from this standpoint.

REFERENCE VEHICLES, DYNAMIC DRIVING CONDITIONS AND MEASUREMENT DATA

Reference Vehicles

In order to compare the available waste heat flows of the different vehicle concepts, two petrol-powered reference vehicles of the compact class were selected. Figure 1 shows the main characteristics of the chosen reference vehicles.

To represent a common conventional vehicle, the Volkswagen Golf VII with a turbocharged engine with 1.2 L displacement was selected. As a hybrid vehicle, the Opel Ampera (Chevrolet Volt) with 1.4 L displacement was chosen. Both vehicles are shown in Fig. 2, while they are being measured on the roller dynamometer test bench of the DLR—Institute of vehicle concepts in Stuttgart.

The Opel Ampera with its power train as a power-split hybrid represents the majority of current plug-in hybrid electrical vehicles (PHEV). Other comparable examples of power-split hybrids are Mercedes C 350e, BMW 330e, Volkswagen Golf GTE and Toyota Prius. The propulsion system of the Opel Ampera is shown in Fig. 3.[8]

The kinematic architecture of the power-split PHEV has a planetary gear set and three clutches. The clutches connect and disconnect the power sources in order to realize different operating modes. To compare the hybrid vehicle with the conventional vehicle, the hybrid vehicle was operated in the charge sustaining mode. In this mode,

	Vehicle type	Battery capacity	ICE	Type of engine	Displacement	Max. Performance	Operating strategy	Transmission	Weight of vehicle	Year of launch	Fuel consumption (measured)	CO_2 emissions (calculated)
	[-]	[kWh]	[-]	[-]	[dm^3]	[kW]	[-]	[-]	[kg]	[-]	[l/100km]	[g/km]
Volkswagen Golf VII	Conv.	-	Turbo (TSI)	4 cyl. in-line	1.197	77	Start-stop	Autom. (DSG)	1300	2012	5.63	131.2
Opel Ampera	Hybrid	16	Otto	4 cyl. in-line	1.398	63	Power-split		1700	2012	6.76*	157.5*

* within the charge sustaining mode

Fig. 1. Main characteristics of the reference vehicles.

Fig. 2. Reference vehicles at the roller dynamometer test bench.

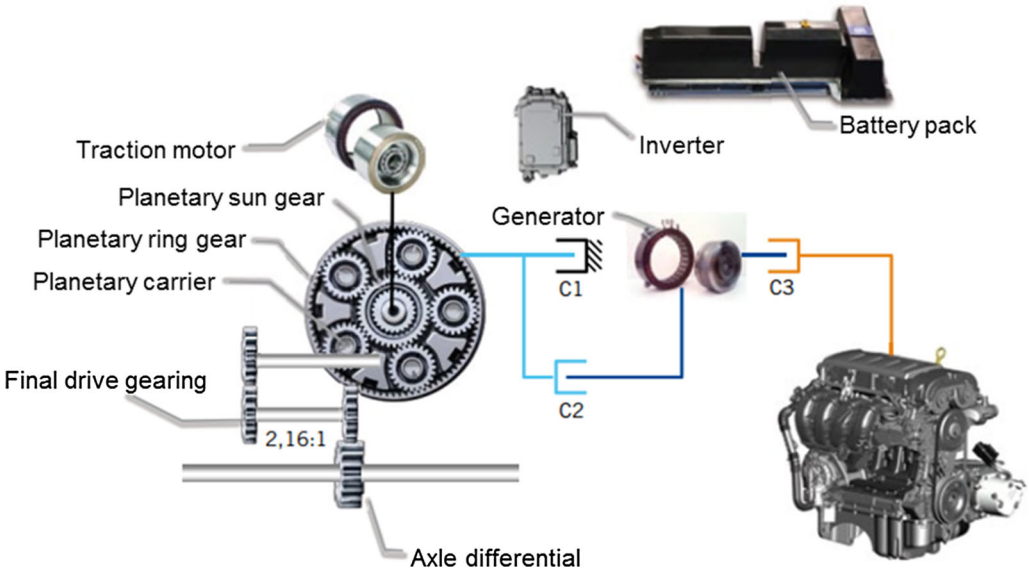

Fig. 3. Propulsion system of the Opel Ampera—Kinematic architecture of the power-split PHEV. (Reprinted with permission of Ref. 8).

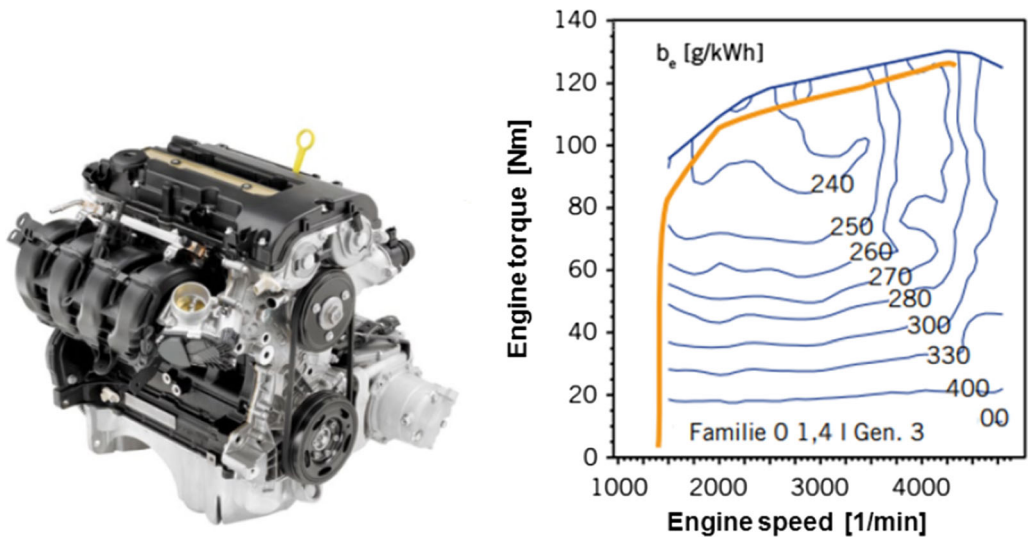

Fig. 4. Internal combustion engine of the Opel Ampera and its operating characteristics, shown in a torque-speed diagram. (Reprinted with permission of Ref. 8)

the cycle is started with an empty traction battery, so that the required energy must be supplied by the combustion engine.

In hybrid vehicles, the combustion engine is operated at higher load points than in conventional vehicles. At these higher load points, the combustion engine has higher efficiencies. As shown in Fig. 4 (orange curve), the combustion engine of the Opel Ampera is operated at various high-load points. Figure 4 also shows that the specific fuel consumption is lower at the high operating points.

Dynamic Driving Conditions

Dynamic driving conditions were chosen in order to show a meaningful comparison of the two propulsion systems. In particular, the worldwide harmonized light duty driving test cycle (WLTC) was selected as part of the related test procedure WLTP.[9]

As shown in Fig. 5, the used WLTC is 1800 s long and has an average speed of 46.5 km/h and a top speed of 131 km/h. For the following comparison, the vehicles were measured at 20°C ambient temperature. The dynamic velocity profile in Fig. 6 shows that a very low load level is required in the first third. A high speed is only driven in the last 323 s of the cycle, in the so-called extra high part.

The velocity profile and the vehicle mass mainly determine the energy required by the propulsion system of the vehicle. As shown in Fig. 1, the mass of the hybrid vehicle is 400 kg higher.

	Time	Distance	Test temperature	Highest speed	Average speed	Highest acceleration	Highest deceleration
	[s]	[km]	[°C]	[km/h]	[km/h]	[m/s²]	[m/s²]
WLTC	1800	23.3	20 / -7	131	46.5	1.8	-1.5

Fig. 5. Dynamic driving conditions of the WLTP driving cycle.

Measurement Data from the Roller Dynamometer

For the following comparison, measurement data from the roller dynamometer test bench were used. The measured fuel consumption for both vehicle concepts is shown in Fig. 1. The value of the hybrid vehicle marked with * refers to the charge sustaining mode.

The exhaust gas temperatures were measured at the point after the catalytic converter. The measurement position used for the Opel Ampera is shown in Fig. 7.

Figure 8 shows the measured exhaust gas temperature and mass flow for the Opel Ampera. It can also be seen from the exhaust measurement data that the combustion engine operates in a hybrid mode. For example, in the first third of the cycle, the exhaust gas mass flow shows that the combustion engine does not cover the low load points as in conventional drive trains. When the combustion engine is used, it varies between different high load points. In these phases, more electrical energy is converted from the fuel and the phases with low load are driven purely electrically. Finally, with the hybrid vehicle in charge sustaining mode, the energy required to move the vehicle within the specified driving cycle is converted from fuel. The difference is that the combustion engine works only at high load points as described above.

POTENTIAL ANALYSIS FOR WASTE HEAT RECOVERY IN VEHICLE APPLICATIONS

In this section, the measured data of the exhaust gas temperatures and mass flows will be compared for the conventional and hybrid vehicles, with the aim of analyzing the potential for waste heat recovery, e.g. with the aid of thermoelectric generators.

Figure 9 shows a comparison of the exhaust gas temperatures and mass flows within the WLTC. It can be seen that the hybrid vehicle has significantly higher exhaust gas temperatures. On the other hand, the maximal reached exhaust gas mass flows over the cycle are slightly lower.

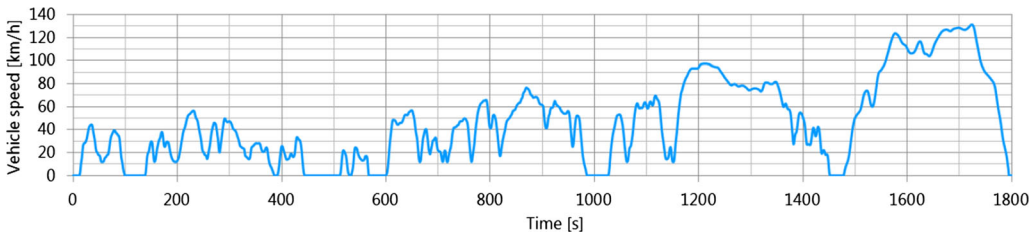

Fig. 6. Velocity profile of the WLTP driving cycle[10].

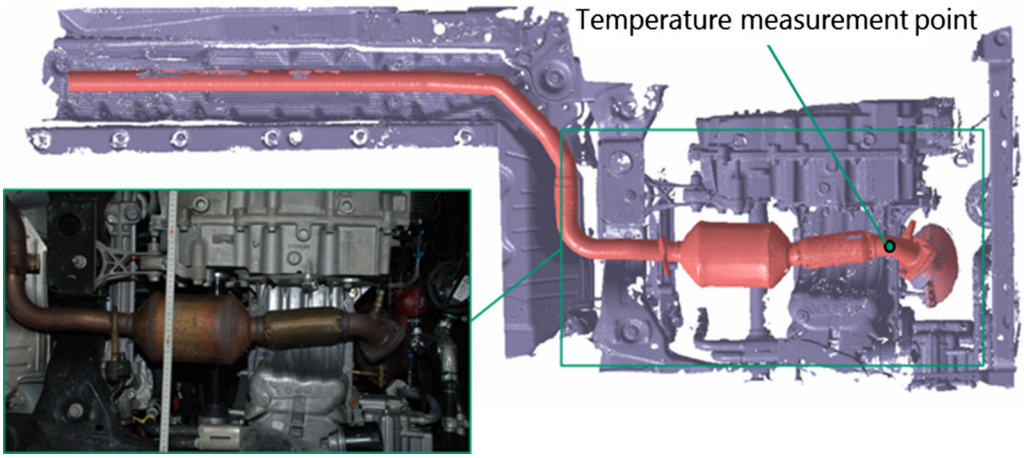

Fig. 7. Measurement position of the exhaust gas temperature after the catalytic converter of the Opel Ampera.

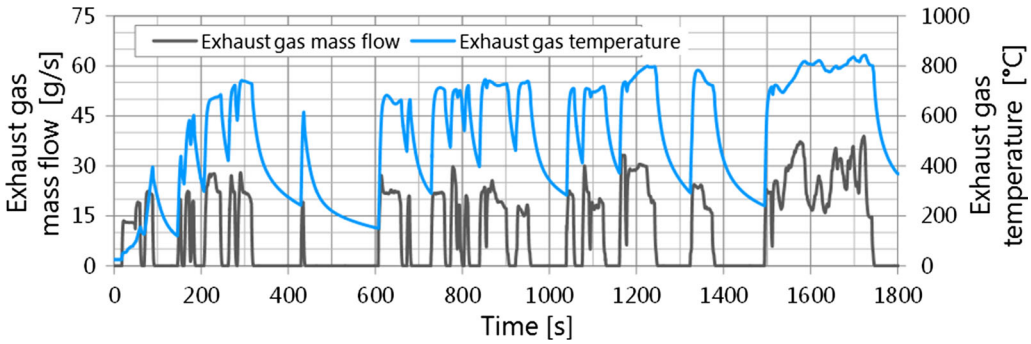

Fig. 8. Measurement data of the exhaust gas mass flow and temperature of the Opel Ampera.

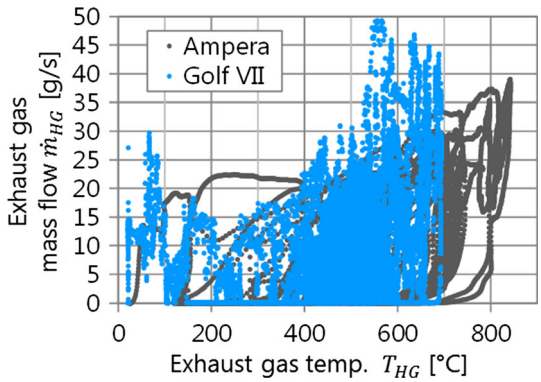

Fig. 9. Comparison of the exhaust gas mass flow and temperature between the two reference vehicles within WLTC.

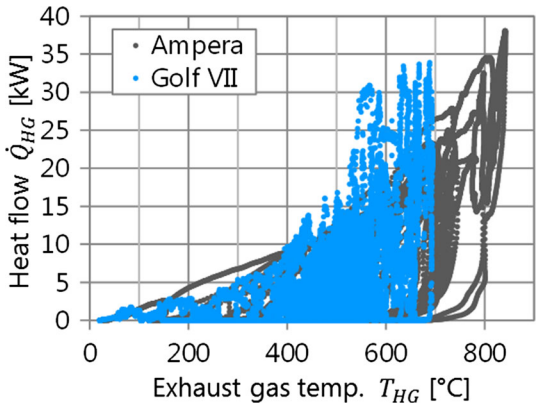

Fig. 10. Heat flow over the exhaust gas temperature for both reference vehicles within the WLTC.

Analysis of the Heat Flow

The calculation of the exhaust gas heat flow ($\dot{Q}_{\mathrm{HG}}$) includes the exhaust gas mass flow ($\dot{m}_{\mathrm{HG}}$) and temperature (T_{HG}) and is carried out according to Eq. 1.

$$\dot{Q}_{\mathrm{HG}} = \overline{c_{p_{\mathrm{HG}}}}\Big|_{T_A}^{T_{\mathrm{HG}}} \cdot \dot{m}_{\mathrm{HG}} \cdot (T_{\mathrm{HG}} - T_A). \qquad (1)$$

However, in addition to the heat flow, the temperature level is important for an efficient use of the waste heat. Therefore, Fig. 10 shows the exhaust gas heat flow over the exhaust gas temperature.

It can be seen that the hybrid vehicle has higher heat flows in the exhaust gas than the conventional vehicle. In addition, these higher heat flows are still at a higher temperature level.

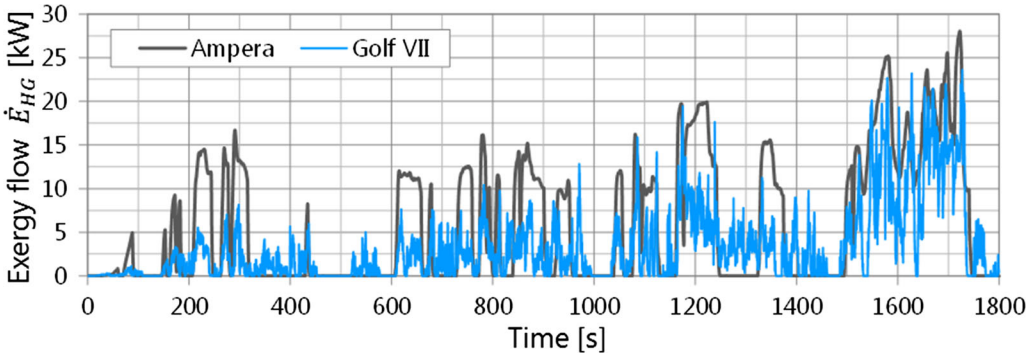

Fig. 11. Exergy flow in the exhaust gas of both reference vehicles within the WLTC.

Analysis of the Exergetic Potential

In order to include the higher temperature level of the exhaust heat flows in the evaluation, the exergy flows ($\dot{E}_{\mathrm{HG}}$) are calculated according to Eq. 2 below. Thereby the exhaust heat ($\dot{Q}_{\mathrm{HG}}$) flow is multiplied with the Carnot efficiency (η_{C}).

$$\dot{E}_{\mathrm{HG}} = \dot{Q}_{\mathrm{HG}} \cdot \eta_{\mathrm{C}}. \tag{2}$$

The Carnot efficiency is calculated according to Eq. 3 from the temperature level of the exhaust gas (T_{HG}) to ambient (T_A).

$$\eta_{\mathrm{C}} = 1 - \frac{T_A}{T_{\mathrm{HG}}}. \tag{3}$$

Thus the exergy flow represents the entire potential for a waste heat recovery system. For example, the conversion efficiency of a thermoelectric generator (TEG) or an organic Rancine cycle (ORC) also depends on the Carnot efficiency.

Figure 11 shows the exergy flows of the two vehicle concepts over time in the WLTC. This clearly reflects the fact that the combustion engine in the conventional vehicle operates at many partial load points, resulting in low exergy flows in the first part of the cycle. In contrast, the hybrid vehicle shows significantly higher exergy flows, especially in the first part of the cycle. These higher exergy flows occur in the hybrid vehicle over a shorter period of time.

An analysis of the absolute frequency of the different exergy flows is shown in Fig. 12. The absolute frequency was calculated over the time of the WLTC by a summation of the amount for each exergy flow level. Figure 12 shows that in conventional vehicles the low exergy flows occur with a very high absolute frequency. The higher exergy flows occur only rarely. On a closer look at Fig. 11, it can also be seen that in the conventional vehicle the high exergy flows occur only in the last part of the cycle (extra high part).

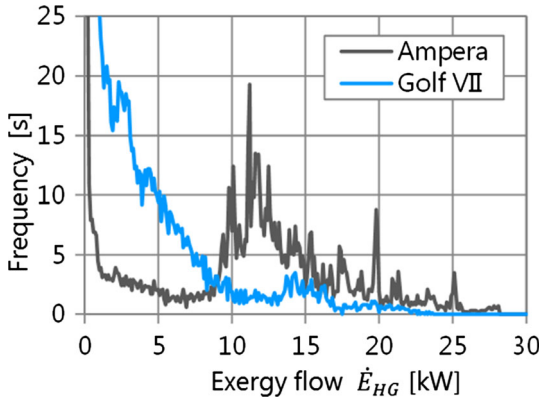

Fig. 12. Distribution of the absolute frequency of exergy flows—both reference vehicles within the WLTC.

	$\dot{Q}_{HG,max}$	$\dot{Q}_{HG,mi}$	$\eta_{c,max}$	$\eta_{c,mi}$	$\dot{E}x_{HG,max}$	$\dot{E}x_{HG,mi}$
	[kW]	[kW]	[-]	[-]	[kW]	[kW]
VW Golf VII	33.9	5	0.697	0.589	23.6	3.2
Opel Ampera	38.1	8.1	0.737	0.584	28.1	5.7

Fig. 13. Results of the exergetic potential analysis within the WLTC.

With the hybrid vehicle, on the other hand, medium to large exergy flows occur with a high absolute frequency. This can be explained by the fact that the combustion engine is operated at higher load points.

The maximum and average values within the WLTC are shown as summary of the analysis in Fig. 13. The average heat flow of the hybrid vehicle's exhaust gas within the WLTC is about 62% higher. Figure 1 shows that the measured fuel consumption of the hybrid vehicle is about 20% higher. This value must be subtracted when comparing the potential. Nevertheless, the average heat flow in the exhaust gas of the hybrid vehicle is still significantly higher than in the conventional vehicle. An explanation for this fact will be given in the following section. In addition, the analysis has shown that the exhaust gas temperatures are

higher in the hybrid vehicle. As a result, the maximum Carnot efficiency is also higher than in the conventional vehicle. However, the average Carnot efficiency in the WLTC is not significantly higher, since the longer standstill phases of the combustion engine reduce it.

Nevertheless, the average exergy flow calculated from the exhaust gas heat flow and the Carnot efficiency is a remarkable 78% higher in the hybrid vehicle. This is due to the fact that in the transient course of the cycle, the high Carnot efficiencies occur together with high exhaust gas heat flows.

ENERGY FLOWS IN CONVENTIONAL AND HYBRID VEHICLES

Here, an explanation will be given for the fact that, in the comparison of the measurement data from the roller dynamometer, the exhaust heat flows are higher in the hybrid vehicle. Even though in this vehicle concept the combustion engine is operated with a higher efficiency, more heat is lost in the exhaust gas. The explanation shall be given generally concerning the thermodynamic relations within an internal combustion engine. Therefore the first law of thermodynamics according to Ref. 11 is mentioned in Eq. 4. In this context, the mechanical work, the wall heat losses and the exhaust gas enthalpy will be discussed.

$$\underbrace{-p\frac{\mathrm{d}V}{\mathrm{d}\varphi}}_{\text{Mechanical work}} + \frac{\mathrm{d}Q_F}{\mathrm{d}\varphi} \underbrace{-\frac{\mathrm{d}Q_W}{\mathrm{d}\varphi}}_{\text{Wall heat losses}} + h_I\frac{\mathrm{d}m_I}{\mathrm{d}\varphi} + \underbrace{h_O\frac{\mathrm{d}m_O}{\mathrm{d}\varphi}}_{\text{Exhaust gas enthalpy}} - h_O\frac{\mathrm{d}m_{\mathrm{Leak}}}{\mathrm{d}\varphi} = \frac{\mathrm{d}U}{\mathrm{d}\varphi} \tag{4}$$

Focusing on the mechanical work, we see that this is higher in the hybrid vehicle because the internal combustion engine is operated at a higher load point. Figure 4 shows that at higher load points the ICE has a lower specific fuel consumption and thus a higher efficiency. On the other hand, the measured values in the exhaust tract show, as already described, higher exhaust gas enthalpy flows.

The first law of thermodynamics is balanced by the fact that the wall heat losses are significantly lower.

Figure 14 shows the wall heat losses exemplary for an internal combustion engine as a function of the engine speed and load according to Ref. 11 It can be seen that in idling and at a medium speed around 26% of the energy supplied by the fuel (Q_F) is lost in the form of wall heat (Q_W). In contrast to this, at full load only 12% of the energy supplied by the fuel are lost as wall heat. Thus in this example the difference in wall heat losses is 14%.

Beyond this general example, the measurement data of the two vehicles in the WLTC will be used for the next step. The measured exhaust gas temperatures, mass flows, speeds and torques of the combustion engine are used. With the help of this data, the energy flows in the conventional and hybrid vehicles were analysed. The mechanical work of the combustion engine was calculated from the torque and the speed. The calculation of the exhaust gas enthalpy is based on Eq. 3 with the measured exhaust gas temperatures behind the catalytic converter. In order to consider the decrease in temperature until the measuring point, the exhaust gas temperature was increased by a maximum of 100 K with a time-dependent compensation to calculate the exhaust gas temperature directly after the engine. For the calculation of the wall heat

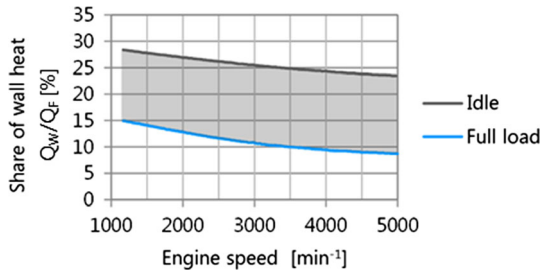

Fig. 14. Share of wall heat losses in relation to the supplied fuel energy and as a function of the load and engine speed. (Data used from Ref. 11)

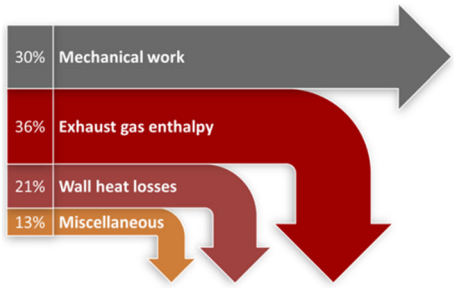

Fig. 15. Energy flow diagram of the conventional vehicle in WLTC average.

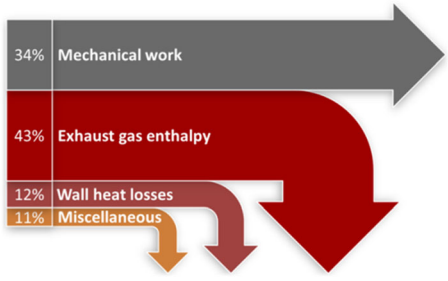

Fig. 16. Energy flow diagram of the hybrid vehicle in WLTC average and operated in the charge sustaining mode.

losses, a function was formed in dependence on load and speed according to Fig. 14, and thus the wall heat losses were calculated for both vehicles.

Figures 15 and 16 summarize the average values in the WLTC. The converted fuel energy, which is calculated from the measured fuel consumption, is used as 100%. The miscellaneous arrow represents the losses neglected in this consideration. These additional losses are based on convection and radiation to the environment, as well as blowby and other heat flows into the coolant. The adjustment was made at this point in order to be able to present a general comparison of the two vehicle concepts based on their three main energy flows.

As a result, Figs. 15 and 16 show that hybrid vehicles lose their highest percentage of waste heat flows via the exhaust system. In relation to the supplied fuel energy, the wall heat losses in the hybrid powertrain are lower, and thus the waste heat in the exhaust tract is higher by 7 percentage points. Also, the efficiency of the combustion engine is 4 percentage points higher in average over the cycle. The higher efficiency of the combustion engine and the higher waste heat flows in the exhaust gas are related. Both result from the fact that the combustion engine is operated at a higher load point. Furthermore, as described in the previous chapter, the exhaust gas temperatures in hybrid vehicles are higher, which means that the exergetic potential is higher in addition to the higher waste heat flows.

The higher potential for waste heat recovery in hybrid vehicles described here results from the fact that the combustion engine is operated at higher load points. This is the case not only in hybrid powertrains. Many other efficiency measures also result in an increase in the load point of the combustion engine, such as down-sizing or cylinder deactivation. This means that, with a wide range of efficiency measures on combustion engines, there is also an accompanying higher potential for waste heat recovery.

CONCLUSIONS

A high potential for waste heat recovery in future vehicles has been shown in this work. In many efficiency measures, the load point of combustion engines is increased in order to improve the efficiency. This is used, for example, in hybrid drive trains as well as for down-sizing and cylinder deactivation. This work demonstrates that at a higher load point the combustion engine has a higher efficiency and, at the same time, the heat losses in the exhaust gas are higher. This has been explained thermodynamically by the fact that the wall heat losses are lower at higher operating points.

In a comparison between two vehicles of the compact class, this relationship was proven on the basis of measurement data from the roller dynamometer test bench. A conventional vehicle (Volkswagen Golf) and a hybrid vehicle (Opel Ampera) were compared. The hybrid vehicle with its as a power-split hybrid power train represents the majority of current plug-in hybrid electrical vehicles (PHEV). The comparison shows that the measured waste heat flow of the hybrid vehicle during operation in the charge sustaining mode is 62% higher. In an additional analysis it was shown that not only the exhaust heat losses themselves are higher in hybrid vehicles, also the temperature level is higher. This results in higher exergy flows in the hybrid vehicle. The analysis showed that the averaged exergy flow within the WLTC is 78% higher for the hybrid vehicle. Accordingly, the potential for waste heat recovery in hybrid vehicles is about 1.8 times higher than in conventional vehicles. Furthermore, an additional heat input from the exhaust system can lead to a high increase in efficiency and comfort due to better thermal management. These effects can be even higher in hybrid vehicles than in conventional vehicles. In order to limit climate change, all promising technologies must be used. As shown, the recovery of waste heat, for example through a thermoelectric generator, can make a decisive contribution in the future.

ACKNOWLEDGMENTS

Open Access funding provided by Projekt DEAL.

OPEN ACCESS

REFERENCES

1. M. Kober, *Holistic Optimization of Thermoelectric Generators for Automotive Applications: Reaching a Cost Benefit Ratio of 81 €/(g/km).* (elib DLR, 2016), https://elib.dlr.de/125922/. Accessed 10 Jan 2019.
2. M. Kober, *Thermoelectric Generators for Automotive Applications: A New Approach to Reach the Cost-Benefit Target.* (elib DLR, 2016), https://elib.dlr.de/115947/. Accessed 10 Jan 2019.
3. M. Kober and H. Friedrich, *Thermoelectric Generators (TEG) with high power density for application in hybrid cars.* (elib DLR, 2016), https://elib.dlr.de/107902/. Accessed 10 Jan 2019.

4. C. Häfele, *Entwicklung fahrzeuggerechter Thermoelektrischer Generatoren zur Wandlung von Abgaswärme in Nutzenergie, Forschungsbericht 2016-08* (Köln: Deutsches Zentrum für Luft- und Raumfahrt, 2016).
5. M. Kober, C. Häfele, and H. Friedrich, *Methodical Concept Development of Automotive Thermoelectric Generators.* (elib DLR, 2016), https://elib.dlr.de/79163/. Accessed 10 Jan 2019.
6. U. Kugler, J. Brokate, C. Schimeczek, and S. Schmid, *Powertrain scenarios for cars in european markets to the year 2040.* (elib DLR, 2017), https://elib.dlr.de/114744/ Accessed 10 Jan 2019.
7. G. Berckmans, M. Messagie, J. Smekens, N. Omar, L. Vanhaverbeke, and J.V. Mierlo, Energies, **10**(9). (2017). https://doi.org/10.3390/en10091314.
8. D. Grebe and L. Nitz, Voltec—the propulsion system for Chevrolet Volt and Opel Ampera. *AutoTechnology (ATZ)* 11, 28–35 (2011).
9. WLTP DHC, *Development of a World-wide Worldwide harmonized Light duty driving Test Cycle (WLTC).* (UN/ECE, 2014), https://www.unece.org/fileadmin/DAM/trans/doc/2014/wp29grpe/GRPE-68-03e.pdf. Accessed 10 Jan 2019.
10. M. Kober, *J. Electron. Mater.* (2020). https://doi.org/10.1007/s11664-020-07966-6.
11. R. Pischinger, M. Klell, and T. Sams, *Thermodynamik der Verbrennungskraftmaschine* (Wien: Springer, 2009).